Entropy of Spatiotemporal Data as a Dynamic Truncation Indicator for Model Reduction Applications

Leonidas G. Bleris and Mayuresh V. Kothare

Abstract— **We have provided a methodology [1] for retrieving spatial and temporal eigenfunctions from an ensemble of data. Focusing on a Newtonian fluid flow problem, we illustrate that the efficacy of these two families of eigenfunctions can be different when used in model reduction projections. The above observation can be of critical importance for low-order modeling of distributed parameter systems in on-line control applications, due to the computational savings that are introduced. For the particular fluid flow problem, we introduce the use of the entropy of the data ensemble as the criterion for choosing the appropriate eigenfunction family. Finally, we examine the use of the entropy as a dynamic truncation indicator.**

I. Introduction

Proper Orthogonal Decomposition (POD) is based on second-order statistical properties, which result in a set of empirical eigenfunctions (also called spatial modes) from a collection of data. These modes are used in a Weighted Residual Method (WRM) [2], [3] to obtain a finite dimensional low-order dynamical system which has the smallest degree of freedom possible. Detailed analysis of the POD-Galerkin projection is provided in [4]. Although the theory behind POD dates back to 1933 [5], recently this method has received substantial attention, primarily because of two factors. Firstly, extracting structural information from large amounts of data has become of growing importance and POD is the optimal empirical method for capturing these features. Secondly, for the application of feedback control to infinite-dimensional Distributed Parameter Systems (DPS) [6] an attractive approach is to approximate the model by some reduced-order model [7] and develop control algorithms for the simplified model.

Even though the efficiency of POD is dependent on the initial data ensemble, there are no a priori rules for the generation of the ensemble. In order to obtain the eigenfunctions a basic assumption is made that the data is fully representative of the temporal progression of the system. Under this assumption (when working in one dimension in space and in time) the pre-dominant approach (see [1] for references) is to obtain spatial eigenfunctions and proceed with the model reduction. In this article we assume that the data ensemble spans the domain both temporally and spatially; thus we can obtain two families of empirical eigenfunctions from the initial data ensemble. One family characterizes the changes in the spatial profile (the spatial eigenfunctions φ) and the other characterizes changes in time (the temporal eigenfunctions ψ) [1]. With the use of an example, we reveal that the temporal eigenfunctions can provide better results in reducing the size of the original model. We illustrate that the entropy of the spatiotemporal data can provide valuable information about the complexity of the spatial and temporal variations (of the original ensemble) separately. Additionally we propose the use of the entropy in order to dynamically reconstruct the data ensemble, providing further computational savings.

In this work, we utilize a fluid flow problem to create the initial data ensemble and we examine the efficiency of the temporal and spatial eigenfunctions when used as basis function for model reduction. This choice can be of critical importance for the quality of the reduced order model and subsequently for on-line control applications. While our study of POD is motivated by the need to apply reduced-order control in a microchemical system (thus the examined microfluidic problem), the results and their implications are broadly relevant to DPS systems which have constraints of high sampling rates for fast on-line model-based control.

II. Construction of the Data Ensemble

For the generation of the data ensemble we use the fluid flow problem of the geometry given in Figure 1.

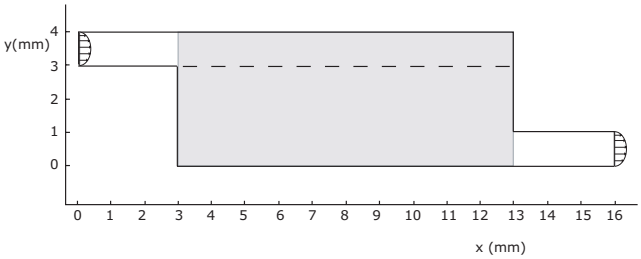

Fig. 1. Geometry examined.

The inlet is located at the top left of the geometry and the outlet on the bottom right. The dynamic model of the fluid flow can be described by the incompressible Navier-Stokes equations:

$$\frac{\partial u}{\partial x} + \frac{\partial v}{\partial y} = 0 \tag{1}$$

Partial financial support for this research from the US National Science Foundation under grants CTS-9980781 ("Engineering Microsystems: XYZ-on-a-chip" program) and CTS-0134102 (CAREER program) is gratefully acknowledged.

Mayuresh V. Kothare is with the Faculty of Chemical Engineering, Lehigh University, Bethlehem, PA, 18015 mayuresh.kothare@lehigh.edu

Leonidas G. Bleris is with the Department of Electrical and Computer Engineering, Lehigh University, Bethlehem, PA, 18015 leb3@lehigh.edu

$$\frac{\partial u}{\partial t} + u\frac{\partial u}{\partial x} + v\frac{\partial u}{\partial y} = -\frac{1}{\rho}\frac{\partial P}{\partial x} + \eta\frac{\partial^2 u}{\partial x^2} + \eta\frac{\partial^2 u}{\partial y^2} \quad (2)$$

$$\frac{\partial v}{\partial t} + u\frac{\partial v}{\partial x} + v\frac{\partial v}{\partial y} = -\frac{1}{\rho}\frac{\partial P}{\partial y} + \eta\frac{\partial^2 v}{\partial x^2} + \eta\frac{\partial^2 v}{\partial y^2} \quad (3)$$

where u and v are the components of the velocity along the x and y axes, P is the pressure, ρ is the fluid density and η the kinematic viscosity. Additionally we define the boundary conditions to be no-slip at the walls and straight out at the outlet (that is the velocity perpendicular to the outlet is zero). The density of the fluid ρ is set at 1000kg/m^3, and the viscosity η at 0.001kg/m·s. In order to create variations in the spatiotemporal velocity profile of fluid we set the inlet velocity relatively high at v_{in}=0.2m/s.

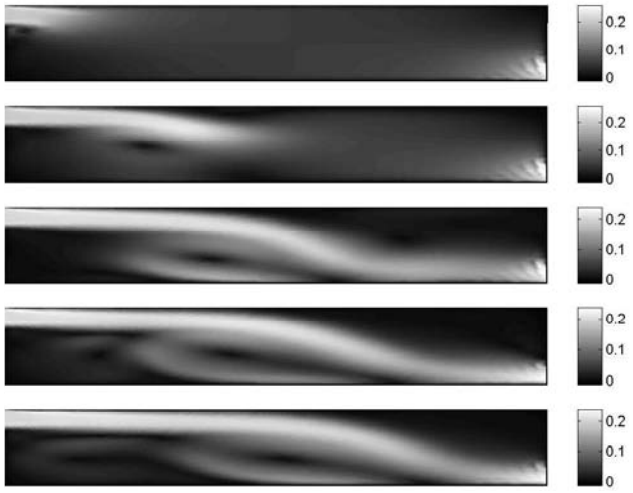

Fig. 2. Velocity solution on the rectangular highlighted area of Figure 1 (from the top: 10^{th}, 50^{th}, 100^{th},150^{th} and 186^{th} sample).

We solve this problem using FEMLAB for the first 0.2s taking $N = 200$ samples temporally; covering the evolution of the fluid flow profile from the initial state to the steady state. We then focus on a domain of interest along the x axis for a given value of y, by measuring the velocity at 200 equally spaced discrete points located along the dashed line of Figure 1. Thus the distance between two discrete points is 50μm. The solution of the velocity profile at the 10^{th}, 50^{th}, 100^{th}, 150^{th} and 186^{th} sample is given in Figure 2. The data ensemble is illustrated in $3D$ in Figure 3. Note that using a finer mesh and lower temporal integration steps did not influence the simulation results. Our goal is to develop a reduced order model to accurately capture the one-dimensional spatiotemporal velocity profile for a given fixed value of y. The behavior of the empirical eigenfunctions throughout the operating region is currently under investigation.

III. Model Reduction

Accurate solutions of distributed parameter systems can be represented as the sum of infinite series. The POD obtained modes are used as basis functions to truncate the

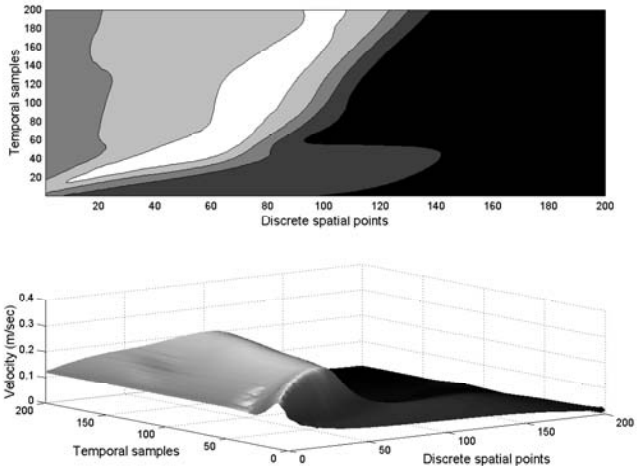

Fig. 3. Data ensemble collected from the cross sectional area (top: contour, bottom: 3D representation).

initial infinite dimensional representation. Using the spatial eigenfunctions the reduced order model $\hat{y}_t(x)$ will be given by:

$$\hat{y}_t(x) = \sum_{n=1}^{\Pi_s} \alpha_n^s(t)\varphi_n(x) \quad (4)$$

and using the temporal eigenfunctions by:

$$\hat{y}_t(x) = \sum_{n=1}^{\Pi_t} \alpha_n^t(x)\psi_n(t) \quad (5)$$

where $\Pi_s < N$ and $\Pi_t < M$ are the number of eigenfunctions used for the reconstruction. The eigenfunction that corresponds to the first eigenvalue (of the ensemble covariance matrix) is considered to be the most "energetic". The "energy" is defined as being the sum of the eigenvalues of the Hermitian matrix [1], and to each eigenfunction we assign an "energy" percentage based on the eigenfunction's associated eigenvalue:

$$E_k = \frac{\lambda_k}{\sum_{i=1}^{N}\lambda_i} \quad (6)$$

Therefore the initial data ensemble can be reduced using only the most "energetic" eigenfunctions. Usually, the sufficient number of eigenfunctions that capture 99% of the system "energy" is used to determine the values of Π_t and Π_s. We will illustrate with the use of an example that for some cases $\Pi_s \neq \Pi_t$. Among all linear decompositions the POD is the most efficient in the sense that for a given number of modes n, the projection on the subspace spanned by the leading n empirical eigenfunctions contains the greatest possible "energy" on average. Thus POD is the optimal empirical method [8] for truncating a high dimensional model. Another significant property of POD is that the following orthogonality relation holds:

$$(\phi_i, \phi_j) \equiv \begin{cases} 0, & i \neq j \\ 1, & i = j \end{cases}$$

where ϕ can be either the temporal ψ or spatial φ eigenfunctions (with the corresponding inner product definition for the temporal and spatial domain). This property is very useful when solving for the coefficients α_n of (4) and (5) analytically; they can be calculated by projecting the data set on each of the eigenfunctions. Finally, using $\hat{y}_t(x)$ we obtain the initial set $\nu_t(x)$ by adding the average of the initial ensemble of snapshots for the spatial or temporal case.

IV. Model Reduction Results

A. Spatial Eigenfunctions as Basis Functions

Using the procedure described in the theory we calculate the spatial eigenfunctions (Figure 4). The energy captured by the first ten eigenfunctions and the total of energy contained is given in Figure 5. We then calculate the coefficients $\alpha_n^s(t)$ projecting the obtained spatial eigenfunctions on the data ensemble:

$$\alpha_n^s(t) = (y_t(x), \varphi_n(x)) \qquad t = 1, ..., N \tag{7}$$

The reduced order representations are obtained using:

$$\nu_t(x) = \nu_{ave}(x) + \sum_{n=1}^{\Pi_s} \alpha_n^s(t)\varphi_n(x) \tag{8}$$

The errors between the original and the reconstructed data sets for different number of modes, are given in Figure 6. The first subplot from the top of Figure 6, is the error resulting using three ($\Pi_s = 3$) eigenfunctions. The second subplot from the top is the reconstruction using four eigenfunctions and so on until $\Pi_s = 7$.

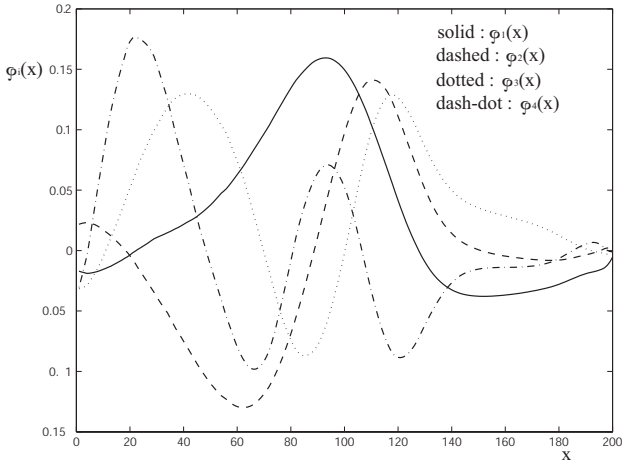

Fig. 4. Spatial eigenfunctions.

B. Temporal Eigenfunctions as Basis Functions

We apply the adjusted method of snapshots to obtain the temporal eigenfunctions (Figure 7). The energy captured by the first ten eigenfunctions and the total energy contained is given in Figure 8. Comparing the two "energy" distributions

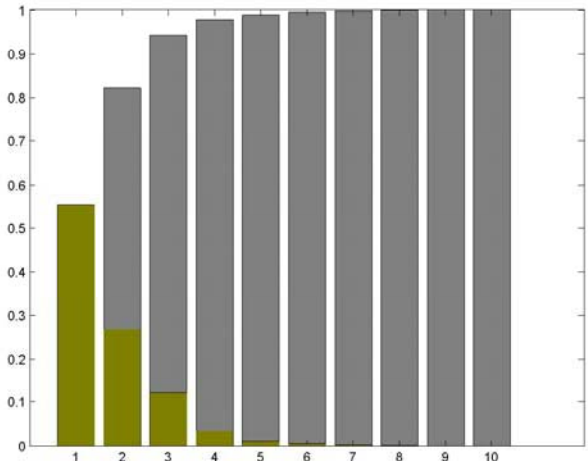

Fig. 5. Energy of spatial eigenfunctions (Green: energy of each mode - Gray: total of energy captured).

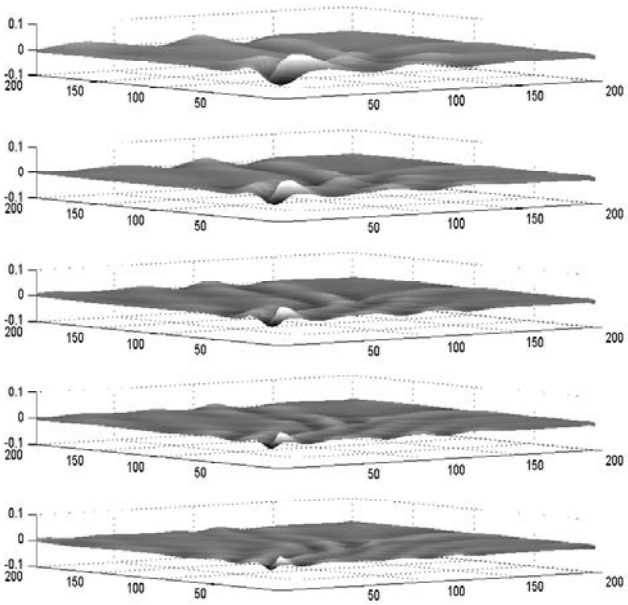

Fig. 6. Error between reconstructed and initial data ensemble, using the spatial eigenfunctions (The top subplot is the error using three eigenfunctions, the second subplot from the top is the error using four eigenfunctions and so on until using seven eigenfunctions).

(of the spatial and temporal case), it becomes evident that the temporal eigenfunctions capture the spatiotemporal changes more efficiently for the particular data ensemble. We calculate the coefficients $\alpha_n^t(t)$ projecting the obtained temporal eigenfunctions to the adjusted data ensemble:

$$\alpha_n^t(x) = (y_t(x), \psi_n(t)) \qquad t = 1, ..., M \tag{9}$$

The reduced order representations of the initial data set can be obtained using the temporal eigenfunction. By adding

the average ensemble we obtain the initial data set:

$$\nu_t(x) = \nu_{ave}(t) + \sum_{n=1}^{\Pi_t} \alpha_n^t(x)\psi_n(t) \qquad (10)$$

The error between the original and the reconstructed data sets for different number of temporal modes, are given in Figure 13. The first subplot from the top of Figure 13, is the error resulting from using three ($\Pi_t = 3$) eigenfunctions. The second subplot from the top is the reconstruction using four ($\Pi_t = 4$) eigenfunctions and so on until $\Pi_t = 7$.

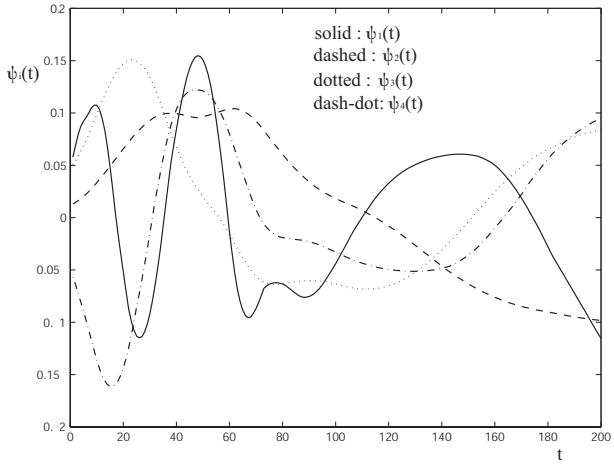

Fig. 7. Temporal eigenfunctions.

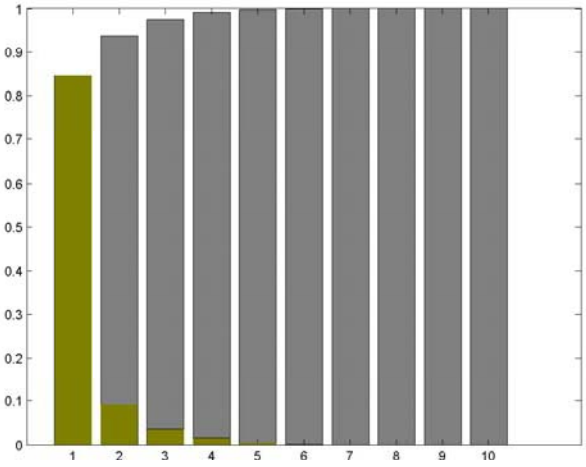

Fig. 8. Energy of temporal eigenfunctions (Green: energy of each mode - Gray: total of energy captured).

C. Data reconstruction simulation results

For the particular data ensemble used, the first spatial eigenfunction (Figure 5) captures 55.4% while the first temporal (Figure 8) eigenfunction 84.4% of the "energy". Most importantly, the first six spatial modes are needed to capture more than 99% of the "energy", while we need

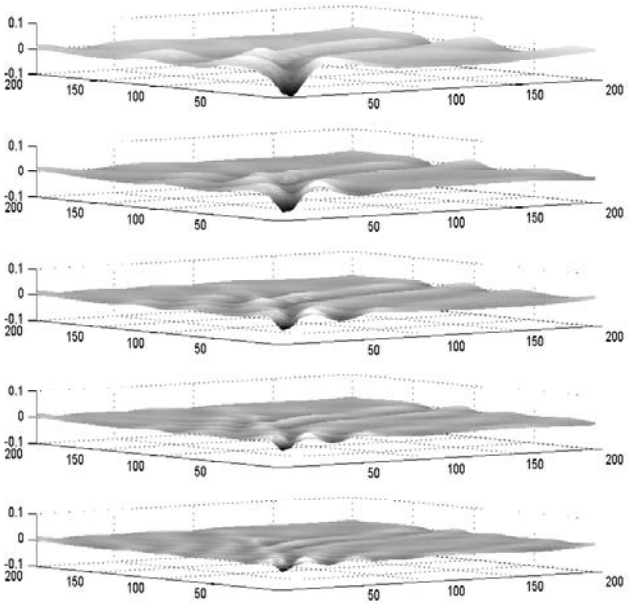

Fig. 9. Error between reconstructed and initial data ensemble, using the temporal eigenfunctions (The top subplot is the error using three eigenfunctions, the second subplot from the top is the error using four eigenfunctions and so on until using seven eigenfunctions).

the first four temporal to achieve the same performance (of capturing the 99% of the "energy"). Therefore the difference of Π_t and Π_s in the particular case is 2. This has an impact on the computational time needed for the calculation of the reduced order model. For the calculation of the reduced order models, we need 0.578s using temporal eigenfunctions and 0.766s using the spatial eigenfunctions (24.54% difference). Thus, even though the difference between the modes required for the reconstruction of the ensemble of Figure 3 is small, the effect on the computational expenses is considerable. Most importantly, the application of a WRM will result to a smaller set of ODEs, providing an advantage towards control applications.

Working towards on-line control of fast DPS, the choice of the appropriate family of basis functions is well justified, even with small differences in their energy content. This becomes particularly important for embedded controllers in microsystem applications, where the sampling time is a major constraint.

V. Entropy of spatiotemporal data

A quantitative measure for the degree of spatial and temporal complexity of a data ensemble can be the "energy" captured by the POD obtained eigenfunctions. The number of eigenfunctions needed to capture 99% of the "energy" depends to the spatiotemporal complexity of the ensemble. Note that in case of underlying patterns only a few modes can be sufficient to capture the dynamics of the system.

The spatiotemporal complexity of the ensemble can be also expressed in terms of the entropy. If the "energy"

is distributed uniformly among all eigenfunctions then the entropy is maximal, equal to one. If only a single mode is excited then the entropy is zero. The entropy of an ensemble of spatiotemporal data is defined [9] by:

$$H = -\frac{1}{log\Delta}\sum_{n=1}^{\Delta} p_n log p_n \tag{11}$$

where Δ is the number of nonzero eigenvalues and p_n are the normalized eigenvalues $p_n = \lambda_n / E$.

To provide the degree of spatial or temporal complexity of the initial data ensemble we use quantities which examine space or time separately. We use the entropy H_ψ that provides the degree of the spatial distribution complexity for each time instant using the temporal eigenfunctions ψ:

$$H_\psi(t) = -\frac{1}{log\Delta}\sum_{n=1}^{\Delta} p_{\psi_n}(t) log p_{\psi_n}(t) \tag{12}$$

where the functions $p_{\psi_n}(t)$, are defined from the eigenvalues λ^t and the temporal eigenfunctions ψ using:

$$p_{\psi_n}(t) = \frac{\lambda_n |\psi_n(t)|}{\sum_{n=1}^{\Delta} \lambda_n |\psi_n(t)|} \tag{13}$$

The entropy H_ψ reveals the contribution of the temporal eigenfunctions at each time sample. The entropy is low when only a few modes are excited.

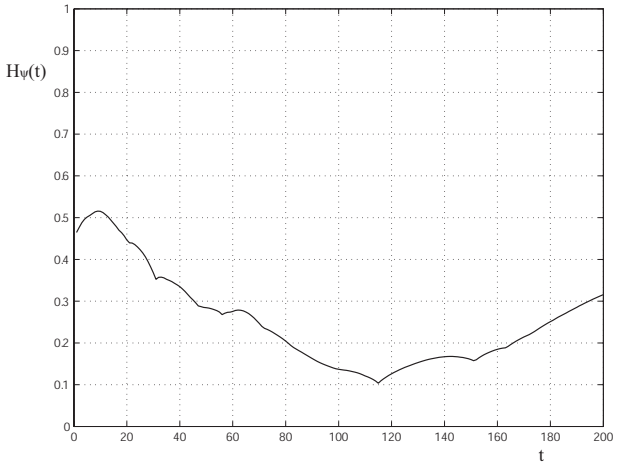

Fig. 10. Complexity in the spatial pattern measured at each time sample.

We also use the entropy H_φ that reveals the degree of complexity of the temporal evolution measured at each spatial position

$$H_\varphi(x) = -\frac{1}{log\Delta}\sum_{n=1}^{\Delta} p_{\varphi_n}(x) log p_{\varphi_n}(x) \tag{14}$$

where the spatial functions $p_{\varphi_n}(x)$ are defined from the eigenvalues λ^s and the spatial eigenfunctions φ using:

$$p_{\varphi_n}(x) = \frac{\lambda_n |\varphi_n(x)|}{\sum_{n=1}^{\Delta} \lambda_n |\varphi_n(x)|} \tag{15}$$

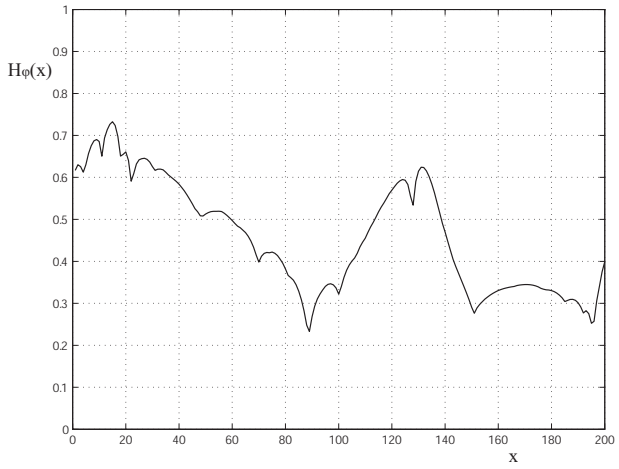

Fig. 11. Complexity in the time series measured at each spatial location.

Using the definitions for the entropies we obtain the degree of spatial or temporal complexity of the initial data ensemble of Figure 3. We notice that the entropy H_ψ (Figure 10) is lower (on average) than the entropy H_φ (Figure 11). We should therefore expect the temporal eigenfunctions to provide a better basis than the spatial eigenfunctions for the model reduction projection.

A. Reconstruction using dynamic truncation

From the preceding analysis we can deduce that the entropies provide a quantitative measure of the degree of participation of the spatial and temporal modes in the dynamical evolution of the system. In [10] the entropy information was used for the stabilization of distributed systems. In this work, we examine the possibility of using the entropies H_φ and H_ψ to dynamically truncate the separate form solutions of distributed parameter systems.

More specifically, for the particular problem examined one can use the entropy H_φ given in Figure 11 to dynamically define $\Pi_s(x)$ (see equation (8)) for each spatial location x, so that only a sufficient number of φ modes are used. Likewise, using H_ψ and $\Pi_t(t)$ for equation (10). We expect a dynamic truncation to minimize the required computational time for the evaluation of the separate forms of the solutions given by equations (8) and (10).

Since the efficacy of the temporal modes is higher than the spatial we examine a dynamic truncation using H_ψ to dynamically define $\Pi_t(t)$ used in equation (10). We assume that the maximum entropy will require the number of eigenfunctions that capture 99% of the energy. For the particular case (Figure 8), we need four temporal eigenfunctions. We use the following ad-hoc *partition rules*:

1. If $H_\psi > 0.3$ use 4 temporal modes.
2. If $H_\psi >= 0.2$ and $H_\psi < 0.3$ use 3 temporal modes.
3. If $H_\psi < 0.2$ use 2 temporal modes.

The resulting number of eigenfunctions to be used as $\Pi_t(t)$ in the dynamic truncation using (10) ar given in Figure 12.

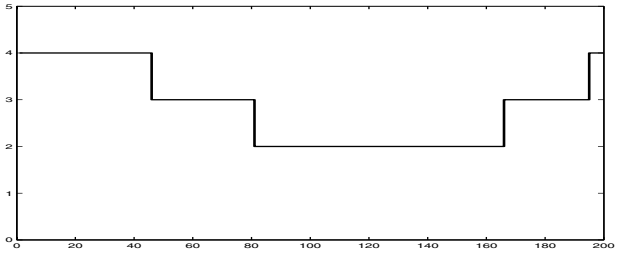

Fig. 12. Number of temporal eigenfunctions ($\Pi_t(t)$) used for each time in the dynamic truncation.

The dynamic truncation has a direct impact on the computational time needed for the calculation of the reduced-order models. For the particular data ensemble used, we need 0.578s using four temporal eigenfunctions, 0.672s using five temporal eigenfunctions and 0.531s using the dynamic truncation (about 20% difference). Note that the number of eigenfunctions used, and thus the computational savings, depend on the partition rules used with the information obtained by the entropies (Figure 12). Therefore one can use the trade-of between the error introduced by the truncation and the computational speed to adjust accordingly the partition rules.

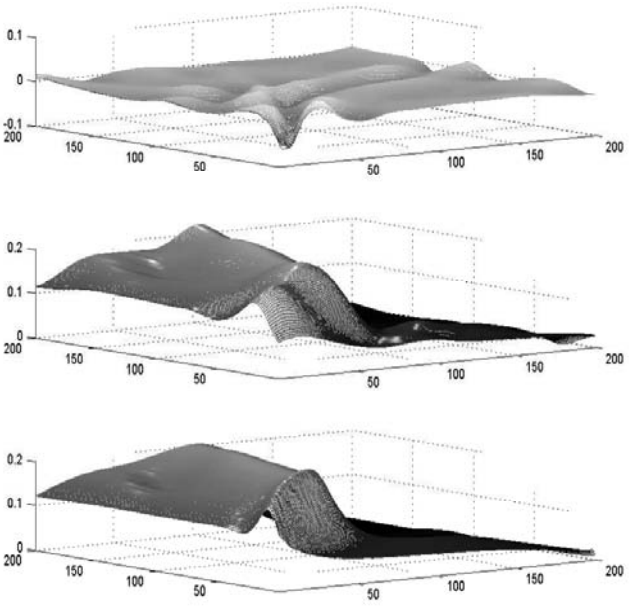

Fig. 13. Dynamic reconstruction of data ensemble using temporal eigenfunctions (The top subplot is the error, the second subplot from the top is the reconstruction, and the bottom subplot is the initial data ensemble).

VI. Concluding Remarks

For the application of POD, under the assumption that a data ensemble captures the dynamics of a system both spatially and temporally, we obtain two families of empirical eigenfunctions. One family characterizes the changes in the spatial profile and the other characterizes changes in time. We have illustrated that these eigenfunctions have different modeling efficacy when used as basis functions for model reduction techniques. While the standard approach for quantifying the spatiotemporal complexity of a data ensemble is the "energy" of the eigenfunctions, we have shown that the entropy can provide valuable insight for the spatial or temporal complexity. We also introduced the concept of dynamic truncation of DPS using the information obtained by the spatial and temporal entropy.

With the use of a fluid flow problem, we showed that for reduced order empirical modeling of DPS towards control applications, the choice of the appropriate eigenfunction family can be of critical importance. Also, the dynamic truncation logic can provide further reduction in the computational costs. The work presented in this paper can be a practical framework towards the development of efficient reduced-complexity controllers, capable of handling the high-dimensional models. The generality of the framework makes it suitable for any DPS which is subject to constraints of high sampling rates for on-line model-based control.

Future work includes the examination of applications, with nonlinear reaction terms that exhibit significantly more complex temporal dynamics. Driven by the results of this work, we expect that the efficacy of the temporal and spatial eigenfunctions (in capturing the dominant dynamics of such a system) will be different. Also, we currently examine the application of feedback control using the information obtained by the entropies, where the control action is centered in "regions of interest" that are defined by the entropies that capture the dominant dynamics of the system.

References

[1] L. G. Bleris and M. V. Kothare. Low-order empirical modeling of distributed parameter systems using temporal and spatial eigenfunctions. *To appear: Computers & Chemical Engineering*, February 2005.

[2] B. A. Finlayson. *The Method of Weighted Residuals and Variational Principles, with Application in Fluid Mechanics, Heat and Mass transfer*, volume 87 of *Mathematics in Science and Engineering, R. Bellman(editor)*. Academic Press, New York, 1972.

[3] Y. Lin, H. Y. Chang, and R. A. Adomaitis. Mwrtools: A library for weighted residual method calculations. *Computers & Chemical Engineering*, 23:1041–1061, February 1999.

[4] P. Holmes, J. L. Lumley, and G. Berkooz. *Turbulence, coherent structures, dynamical systems and symmetry*. Cambridge monographs on Mechanics. Cambridge University Press, 1996.

[5] H. Hotelling. Analysis of a complex of statistical variables into principle components. *Journal of Educational Psychology*, 24:417–441, 498–520, 1933.

[6] P. D. Christofides. *Nonlinear and Robust Control of PDE Systems*. Birkhäuser, Boston, MA, 2001.

[7] S. Y. Shvartsman and I. G. Kevrekidis. Nonlinear model reduction for control of distributed parameter systems: A computer assisted study. *AIChE Journal*, 44:1579, 1998.

[8] J. L. Lumley. *Stochastic Tools in Turbulence*. Academic Press, New York, 1970.

[9] P. Kolodner, S. Slimani, N. Aubry, and R. Lima. Characterization of dispersive chaos and related states of binary-fluid convection. *Physica D*, 85:165–224, 1995.

[10] A. A. Alonso and B. E. Ydstie. Stabilization of distributed systems using irreversible thermodynamics. *Automatica*, 37:1739–1755, 2001.